Failure Analysis of a Hot Forged SAE 4140 Steel Kingpin

J.B. Marcomini[1*], C.A.R.P. Baptista[2], J.P. Pascon[3], R.L. Teixeira[4], P.C. Medina[5]

[1,2,3]Department of Materials Engineering, EEL/USP, University of São Paulo, Lorena/SP, BRAZIL
*Email: jmarcomini@usp.br
[4,5]Bardella S.A. Mechanical Industries, Guarulhos/SP, BRAZIL

Abstract— *The fifth wheel and kingpin connection system, a critical part of heavy vehicles, provides the link of tractor and trailer. The kingpin is usually manufactured by hot forging. A part manufactured by this process was assembled in a fifth wheel of an off-road truck and presented an early failure. The truck was used in a quarry until the kingpin failure, three months later. One process issue that can occur in hot forged products is a poor grain structure due to overheating, burning and cavitation. The Scanning Electron Microscopy (SEM) analysis of the failed part showed the presence of cavitation. However, the failure analysis results evinced that cavitation was not the main cause of the fracture, but a combination of wear, impact fatigue and overload.*

Keywords— *cavitation, failure analysis, hot forged steel, kingpin, overload.*

I. INTRODUCTION

The kingpin coupled to fifth wheel is extensively employed in heavy articulated vehicles to link the towing vehicle to the trailer. The kingpin is fastened in the trailer and it is coupled into the fifth wheel of a tractor. The horizontal load is transmitted from tractor to trailer through the kingpin positioned at the center of the fifth wheel. Hot forging from a steel bar is usually the adopted process to produce this part. Forged products may present the cavitation (grain boundary voids) phenomenon when the steel is preheated to a high temperature (usually > 1200°C) prior to hot working, or when a certain amount of non-homogeneity occurs in the chemical composition of the steel, or even due to problems with the die leading to a non-uniform deformation. Lubrication problems may also lead to grain burning. Thus, local melting can occur at the austenite grain boundaries as a result of segregation of P, S or C. According to ASM Metals Handbook, Vol.11 [1], *"cavitation or ductile rupture is the more dominant mode of ductile fracture when working temperatures are higher than one-half the melting point of a given material"*. Because of the too many parameters that may cause grain burning, it is not a very infrequent problem, and may affect significantly the service performance of the part.

A kingpin was processed by hot forging of a hot rolled 88,90mm round bar of SAE 4140 steel. The part was machined and thermal treated by quenching and tempering. The kingpin was assembled into a fifth wheel of an off-road truck. The truck was used in a quarry until the kingpin failure, after three months. The part fractured in two pieces that are shown in Fig. 1. No other kingpin from same lot was reported do fail since then. An analysis of the failed kingpin is performed in this paper.

| **(A)** | **(B)** |

FIGURE 1. IMAGES OF TOPSIDE (A) AND UNDERSIDE (B) OF THE FRACTURED KINGPIN.

II.   MATERIAL AND METHODS

In order to investigate the cause of the failure, some analyses were performed. The kingpin material characterization was performed by chemical analysis and metallographic and hardness tests. The fracture surface was investigated by scanning electron microscopy (SEM). A stress analysis was carried out using the Finite Element Method (FEM) for the purpose of investigating the possible effects of service loads on the deformation behavior of the kingpin.

III.   MATERIAL CHARACTERIZATION

3.1   Chemical Composition of the Steel

Chemical analysis was performed based on ASTM E 350 [2]. The chemical composition of the steel is presented in Table 1 and is in accordance to SAE J 404 Standard [3].

TABLE 1
CHEMICAL COMPOSITION OF THE STEEL (%WT)

C	Cr	Mn	Mo	Si	S	P
0.40	1.10	0.86	0.17	0.31	0.016	0.011

3.2   Analysis of Microstructure

An optical microscopy metallographic analysis and SEM and X-ray energy dispersive spectrum (EDS) analyses were performed in order to observe the microstructure. Samples were taken from a region about 5 mm under the fracture surface of the kingpin. The polished surface of one sample was etched with nital 3% in order to investigate the microstructure and the other sample was etched with picral 2% in order to observe the prior-austenite grain boundaries. The optical microscope images are shown in Fig. 2 and Fig. 3. The steel microstructure is composed by tempered martensite and bainite. Cavitation and sulfide inclusions can be seen in Fig. 3. Figure 4 is a SEM image in which the cavitation in prior-austenite grain boundaries and MnS inclusions can be observed. The composition of the inclusions was confirmed by the EDS analysis. A mechanism that occurs during the cavitation phenomenon is the dissolution of the manganese sulfide inclusions and subsequent precipitation as globular particles upon cooling. Then a new distribution of MnS forms and it is not uniform, such as a cluster around the cavity.

FIGURE 2. OPTICAL MICROSCOPE IMAGE OF THE KINGPIN STEEL MICROSTRUCTURE SHOWING TEMPERED MARTENSITE AND BAINITE. ETCHANT: NITAL 3%.
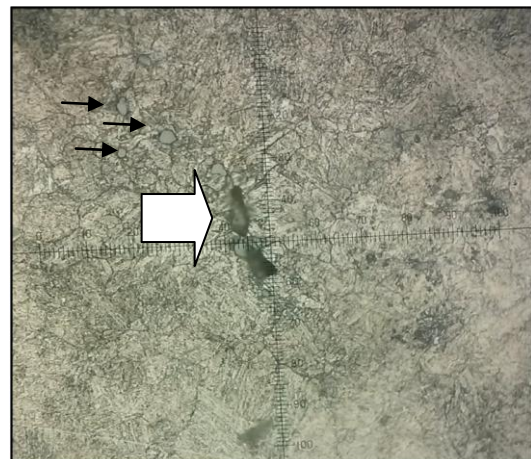

FIGURE 3. OPTICAL MICROSCOPE IMAGE OF THE KINGPIN MICROSTRUCTURE SHOWING PRIOR AUSTENITIC GRAIN BOUNDARIES. GRAIN SIZE: BETWEEN 5 AND 6 ACCORDING TO ASTM E 112 [4]. THE THICK ARROW SHOWS CAVITATION AND THIN ARROWS SHOW SULFIDE INCLUSIONS. ETCHANT: PICRAL 2%.
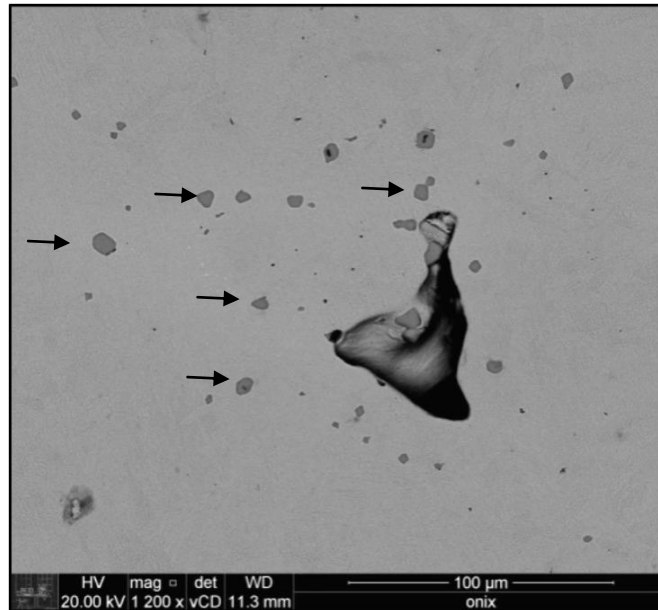
FIGURE 4. SEM IMAGE OF THE KINGPIN. THE THICK ARROW SHOWS CAVITATION AND THIN ARROWS SHOW MANGANESE SULFIDE INCLUSIONS AROUND CAVITATION.

3.3   Hardness Test

Rockwell C hardness measurements were performed in five points of the kingpin cross section from the surface to the center. The test method was based on ASTM A370 [5]. The average hardness value was (36,0+/- 0,5) HRC on the surface, (35,0+/- 0,5) HRC on the half radius and (33,0+/- 0,5) HRC on the center. The found hardness values are compatible with the microstructure and in accordance to the producer's database for this steel.

IV.   FRACTOGRAPHIC ANALYSIS

4.1   Fracture Surface

Figure 5 shows the underside of fractured kingpin with some wear points and pits that may be caused by a combination of contact fatigue, with rolling and sliding, and impact fatigue mechanisms) [1]. Figure 6 shows the fracture surface of the underside of fractured kingpin. The picture plane is normal to the kingpin axis. The contour of the fractured piece, instead of presenting the circular shape of the original kingpin cross-section, is quite irregular, showing evidence of severe deformation. The subsurface fracture origin on the wear region can be observed in Fig. 7.
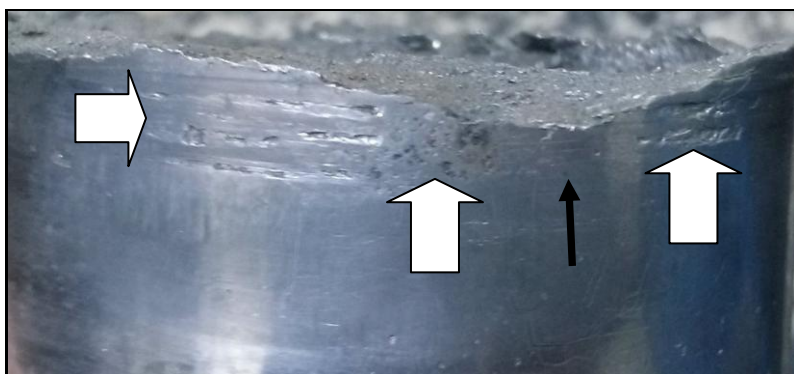

FIGURE 5. IMAGE OF UNDERSIDE OF FRACTURED KINGPIN. THICK ARROWS SHOW WEAR AREAS. THIN ARROW SHOWS THE FRACTURE ORIGIN.

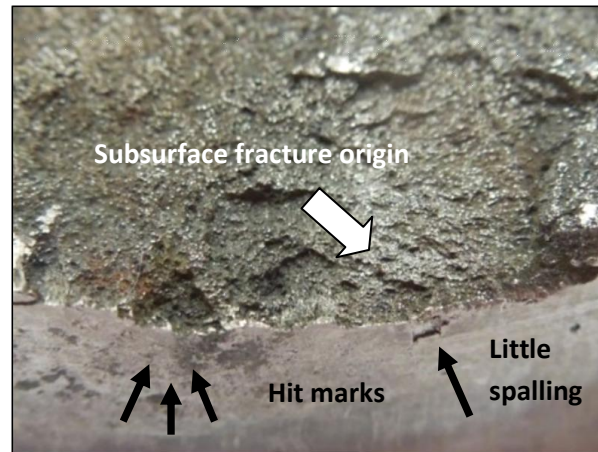**FIGURE 6. IMAGE OF THE FRACTURE SURFACE OF THE UNDERSIDE OF FRACTURED KING PIN. THE ARROW SHOWS THE FRACTURE ORIGIN.**

FIGURE 7. FRACTURE SURFACE OF THE KINGPIN. THICK ARROW SHOWS THE FRACTURE ORIGIN AND THIN ARROWS SHOW THE SPALLING AND HIT MARKS.

4.2 SEM Fracture Surface Analysis

Scanning electron microscopy (SEM) analysis was performed on the kingpin fracture surface. Fig. 8 shows the fracture mechanism next to the fracture origin. The main fracture mechanism observed is quasi-cleavage [6], which is a possible fatigue propagation mechanism for the SAE 4140 steel in as verified by Vargas-Arista et al [7]. There is no precipitation in the subsurface fracture origin. The fracture propagation mechanism changes along the fracture surface to a mixed mechanism of dimples and a few regions of intergranular fracture (Fig. 9).
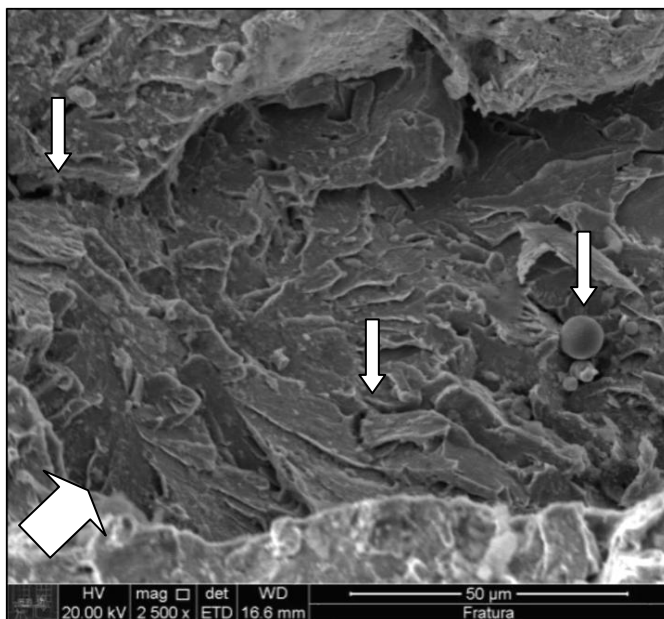

FIGURE 8. SEM IMAGE OF FRACTURE SURFACE OF KINGPIN, NEXT THE FRACTURE ORIGIN, SHOWING QUASI-CLEAVAGE FRACTURE MECHANISM. THICK ARROW SHOWS THE FRACTURE ORIGIN. THIN ARROWS SHOW A CEMENTITE PARTICLE, IDENTIFIED BY EDS (X-RAY ENERGY DISPERSIVE SPECTRUM), AND SECONDARY CRACKS.
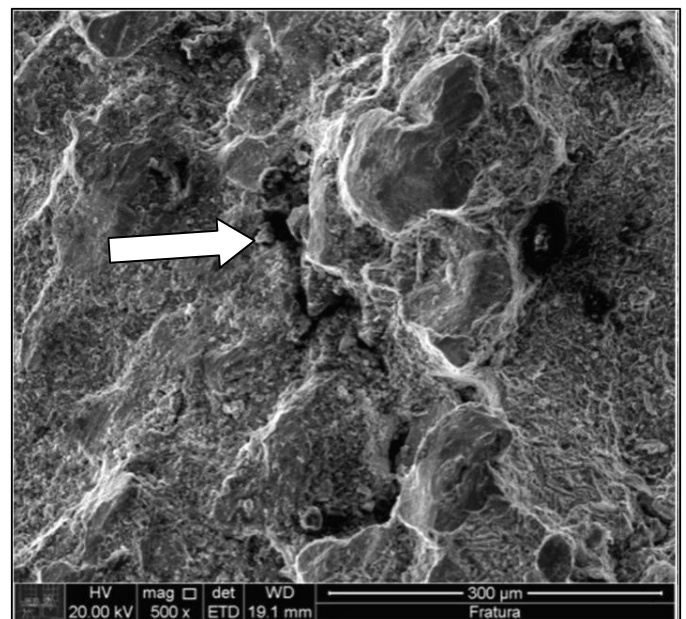

FIGURE 9. SEM IMAGE OF FRACTURE SURFACE OF KINGPIN, FAR FROM THE FRACTURE ORIGIN, SHOWING A MIXED FRACTURE MECHANISM: DIMPLES AND A FEW OF INTERGRANULAR MECHANISM. ARROW SHOWS AN INITIAL CAVITATION.

V.   FINITE ELEMENT ANALYSIS

A numerical model was employed in order to analyze the effect of the service loads on the kingpin mechanical behavior. The geometry and the loading conditions are depicted in Fig. 10. The value of the applied force was obtained from the finite element analysis performed by Shoffner [8], which developed a model in order to study the coupling reactions between the fifth wheel and the kingpin. In that work, the impact force acting on the kingpin reaches a maximum of 37 ton. In the present analysis, due to the possibility of the truck riding on an uneven ground, the adopted force is 40 ton. As one can note in Figure 5.1, the load is uniformly distributed over a lateral surface. With respect to the constitutive law, the material is assumed to be linearly elastic with isotropic hardening behavior described by the Swift model, see equation (1). The material's properties are the following: Young's Modulus $E = 200\ GPa$; Poisson's ratio $v = 0,30$; Swift model's coefficients $K = 1.57\ GPa$; $\varepsilon_0 = 0.0045810633$ and $n = 0.10$. The Swift model and the initial yield stress limit are, respectively:

$$\sigma_Y = K\left(\varepsilon_0 + \kappa\right)^n \Rightarrow \left(\sigma_Y\right)^0 = 916.21 MPa \tag{1}$$

where κ is the isotropic hardening parameter. Moreover, the J_2-flow theory is employed: von Mises yield criterion and associative plastic flow rule (see, among many others, Khan and Huang, 1995 [9]).
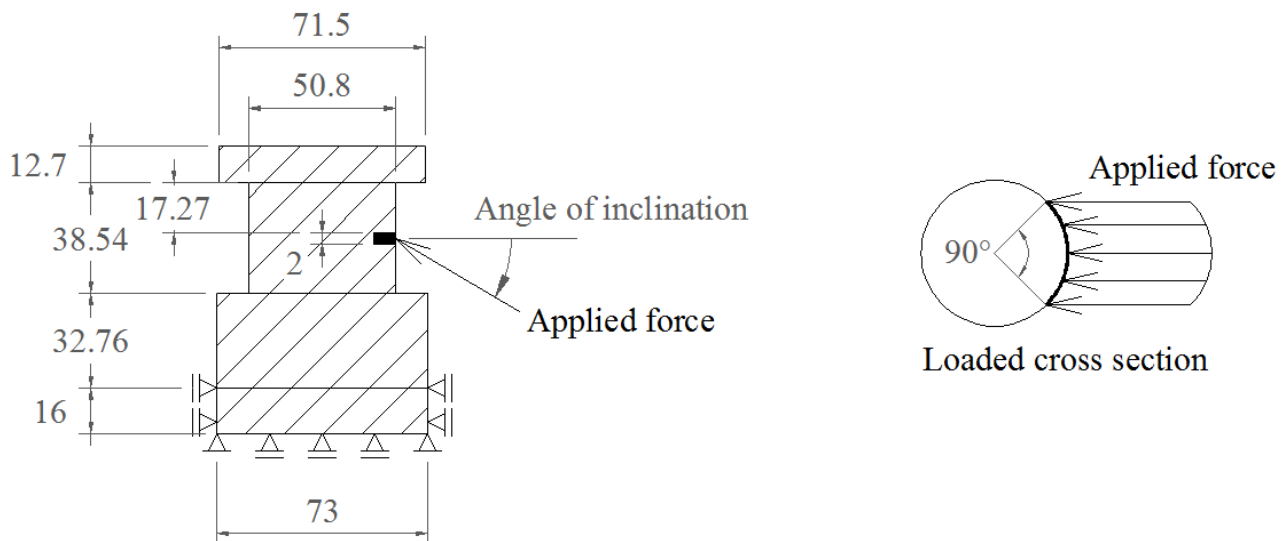

FIGURE 10. FINITE ELEMENT MODEL OF THE KINGPIN (dimensions in mm).

Regarding the numerical model, the finite element mesh is more refined around the critical regions, i.e., near the load and near the diameter discontinuities. The computer code employed has been developed by one of the authors and applied in numerous studies (see, for instance, Pascon and Coda, 2013 [10], which analyzed the mechanical behavior of elastoplastic materials via solid tetrahedral finite elements). The resultant mesh has 1327 nodes and 834 solid tetrahedral finite elements of quadratic order.

Altogether, seven problems were simulated with the numerical model described above, varying the angle of load inclination showed in Fig. 10. The use of different angles is because of the problem complexity resulting from the service conditions in a quarry. When the truck wheel step over a stone or other ground irregularity, the vertical component of the kingpin load may increase, but the true angle of inclination is very difficult to be obtained, as it depends on the truck speed, the irregularity size and the fifth wheel damping system. According to Fig. 11 and Fig. 12, as the angle of inclination with respect to the horizontal direction increases, the von Mises stress and thus the plastic strains increase too. These results reinforce the idea that the use of the truck in such severe operation conditions like those present in a quarry may result in impact stresses leading to plastification, which in turn increases the strains and, thus, the clearance between the fifth wheel and the kingpin (see Fig. 11). Under these conditions, the impact between such components becomes more and more severe.

As expected, the von Mises stress and, thus, the plastification are higher at the region around the applied force (see Fig. 13). This fact is in accordance with the failure analysis performed in the present study, as it confirms the occurrence of plastic (or ductile) deformation at the lateral surface of the kingpin.
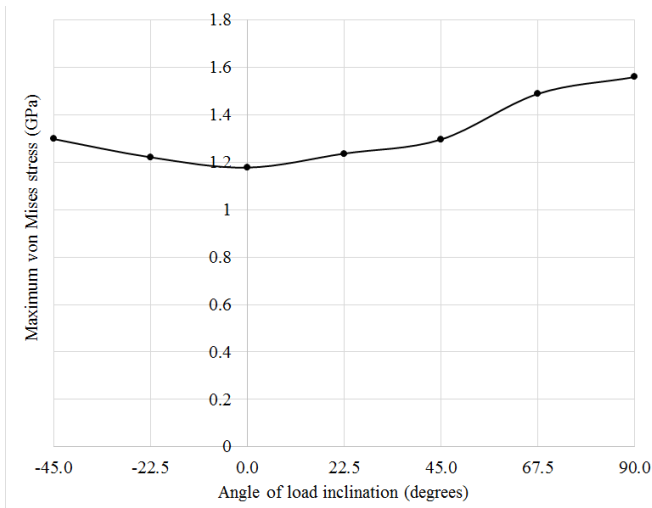
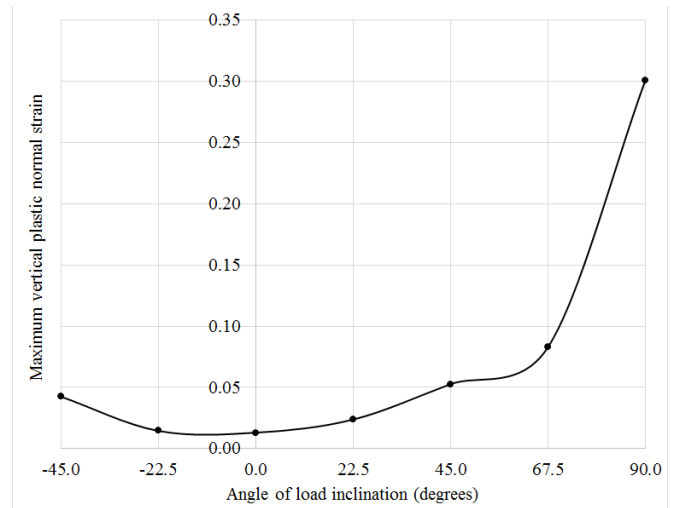**FIGURE 11. MAXIMUM VON MISES STRESS VERSUS THE ANGLE OF LOAD INCLINATION.**

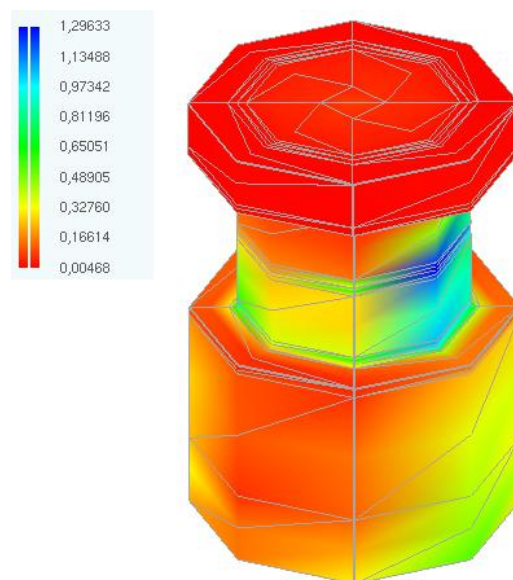**FIGURE 12. MAXIMUM VERTICAL PLASTIC NORMAL STRAIN VERSUS THE ANGLE OF LOAD INCLINATION.**

FIGURE 13. VON MISES STRESS (GPA) FOR THE CASE IN WHICH THE LOAD INCLINATION ANGLE IS 45º.

VI.   DISCUSSION

The image in Fig. 6 shows that global behavior of the part was ductile because of the amount of deformation that occurred on the circumference of kingpin cross section. This fact is in accordance to the surface hardness measured (36 HRC) which is not a brittle condition for this kind of steel. The numerical analysis was able to predict the plastic deformation behavior in the kingpin surface due to the severe service conditions. The random nature of the applied loads and changes in loading point due to maneuvering justify the irregular deformation pattern observed in the kingpin cross section. It was observed that the fracture origin is next a region with wear aspect and pits. In addition, the failure origin is subsurface which leads to the conclusion that the cause of the crack nucleation involves a kind of contact fatigue and impact fatigue.

The contact fatigue theory states that sliding contact fatigue presents the tangential forces and thermal gradient caused by friction, in addition of normal contact stresses. These conditions alter the magnitude and distribution of stresses on and below the contact area. The critical alternating shear stress increases and is moved, which leads to the subsurface crack nucleation and it propagates in a shallow angle to the surface. The pits are formed when the cracks are connected to the surface by secondary cracks [1]. The delamination theory [11] may be applied for fretting and contact fatigue mechanism. This theory states that because of the higher density of dislocations under the surface, this region may suffer strain hardening and the

critical stress occurs rather in this site. On the other hand, it is well known that the repetition of impulsive loads can cause the failure of machine parts by impact fatigue [12].

Maccagno et al [13] performed a failure analysis of the kingpins of two trailers fractured of about 4 to 6 months in service. The fracture surfaces of the kingpins exhibited an oxidized, dark region indicative of high temperature exposure. The fracture propagation mechanism was essentially intergranular. Subsequent analysis concluded that cracks present in the defective kingpins prior to their installation on the trailers had formed during the forging operation and grew during service until catastrophic failure. Solidification shrinkage cavities and MnS inclusions were found throughout the fractured regions of the kingpins. In the present case, the fracture surface mechanism is very different.

The ductile (plastic) deformation of the kingpin cross section possibly enabled the subsequent occurrence of impact fatigue. This deformation caused a clearance between the fifth wheel and kingpin which was the sufficient condition to enable impact loads to occur. The plastic deformation of materials under impact fatigue mainly concentrates around the points of impact loading [14]. Furthermore, the obliquity of the impact, as considered in the numerical analysis, as a consequence of the ground irregularities was considered by Svenzon [15] of fundamental importance for the creation of impact fatigue failure. The observed pits show a peculiar brittle aspect of little spalling that could be caused by an impact against a hardened case such as a martensitic microstructure (Fig. 2 and Fig. 7).

The brittle appearance along the fracture surface (Fig. 6) suggests that, besides the ductile fracture aspect of external surface of king pin, some kind of local embrittlement occurs. This embrittlement could not be caused by cavitation phenomenon because the fracture propagation mechanism is not intergranular, especially in the area next to the fracture origin. The transgranular fracture propagation mechanism next to the fracture origin is common when there is any kind of overload. The finite element analysis showed the possibility of overload occurrence. The inclusion clusters are not the main cause of the nucleation of fatigue crack because the fracture origin does not show any dimples. The cavitation and the manganese sulfide precipitation could contribute to the propagation but they are not the root cause of the failure. Moreover, the tendency to exhibit cleavage rather than a ductile fracture mode is one of the main features of impact fatigue of steels [16]. Then, the observed embrittlement mechanism could be due to impact fatigue [17].

Impact test was performed with samples with presence of cavitation in order to investigate its effect on steel toughness. The results of the impact tests show a 30 J absorbed energy average, which is a suitable result for the 4140 steel quenched and tempered for 36HRC, presenting a mixed microstructure of martensite and bainite. This result is in accordance to the database of the company that supplied the steel applied in the kingpin. In this specific case, the loss of toughness due to the cavitation phenomenon was not detected or it was not so intense.

VII.   CONCLUSION

Summarizing the facts, the truck was used in a quarry under severe operation conditions, riding on an uneven ground, which caused overloads on the fifth wheel coupling. The overloads were transmitted to the kingpin causing the external surface deformation which lead to a clearance formation. The random nature of the applied loads and changes in loading point due to maneuvering justify the irregular deformation pattern observed in the kingpin cross section. This scenario was sufficient to allow the occurrence of contact-fatigue and impact-fatigue mechanisms. Moreover, the finite element analysis performed here corroborates the occurrence of plastic (or ductile) deformation at the lateral surface of the king pin in the case of those severe conditions. The cavitation observed in the kingpin material was not the main cause of the failure but just contributed for the fracture propagation.

REFERENCES

[1] ASM HandbooK, Failure Analysis and Prevention (2002), 11.

[2] ASTM E 350, Standard Test Methods for Chemical Analysis of Carbon Steel, Low-Alloy Steel, Silicon Electrical Steel, Ingot Iron, and Wrought Iron (2000).

[3] SAE J 404 Standard, Chemical Compositions of SAE Alloy Steels (2009).

[4]   ASTM E 112, Standard Test Methods for Determining Average Grain Size (2006).

[5]   ASTM A 370, Standard Test Methods and Definitions for Mechanical Testing of Steel Products (2007).

[6]   Hull, D., Fractography: observing, measuring and interpreting fracture surface topography, Cambridge University Press, 1999. 366p.

[7]   Vargas-Arista, B., Teran-Guillen, J., Solis, J., García-Cerecero, G., Martínez-Madrid, M. Normalizing Effect on Fatigue Crack Propagation at the Heat-affected Zone of AISI 4140 Steel Shielded Metal Arc Welding, Materials Research (2013), 16(4): 772.

[8]   Shoffner, B. W., Development and validation of a finite element analysis model used to analyze coupling reactions between a tractor's fifthwheel and a semitrailer's kingpin, Master Thesis, The Pennsylvania State University, The Graduate School, College of Engineering (2008).

[9]   Khan, A. S., Huang, S. Continuum Theory of Plasticity. New York: John Wiley & Sons, Inc., 1995. 421p.

[10] Pascon, J. P., Coda, H. B., Large deformation analysis of elastoplastic homogeneous materials via high order tetrahedral finite elements, Finite Elements in Analysis and Design (2013), 76: 21–38.

[11] Suh, N.P. The Delamination Theory of Wear, Wear (1973), 25:111.

[12] Iguchi, H., Tanaka, K., Taira, S. Failure Mechanisms in Impact Fatigue of Metals. Fatigue of Engineering Materials and Structures, v.2, (1979) p. 165-176.

[13] Maccagno, T.M., Jonas, J.J., Yue, S., Thompson, J.G. Failure of trailer kingpins caused by overheating during forging. Handbook of Case Histories in Failure Analysis, Volume 2, K.A. Esaklul, editor, (1993), p.53-57.

[14] Yu, J., Liaw, P.K., Huang, M. The Impact-Fatigue Fracture of Metallic Materials. JOM, Journal of the Minerals, Metals & Materials Society, 1999, p.15-18.

[15] Svenzon, M. Impact Fatigue of Valve Steel. In: Proc. of International Compressor Engineering Conference, Purdue University, 1976, p.65-73.

[16] Johnson, A.A., Storey, R.J. The Impact Fatigue Properties of Iron and Steel. Journal of Sound and Vibration, v.308,(2007), p.458-466.

[17] Triantafyllidis, G. K., Kazantzis, A. V., Drambi, E. J., El-Aour Sami, Kalantzis, A. I., Fracture Characteristics of Torsion-Bending Fatigue and Impact Fatigue Failure of Two Steel Pins in a Crawler Excavator, J Fail. Anal. and Preven. (2009), 9:23.